Tropical Cyclone Kinematic Structure Retrieved from Single-Doppler Radar Observations. Part II: The GBVTD-Simplex Center Finding Algorithm

WEN-CHAU LEE

National Center for Atmospheric Research, Boulder, Colorado*

FRANK D. MARKS JR.

NOAA/AOML/Hurricane Research Division, Miami, Florida

(Manuscript received 10 May 1999, in final form 12 August 1999)

ABSTRACT

This paper is the second of a series and focuses on developing an algorithm to objectively identify tropical cyclone (TC) vorticity centers using single-Doppler radar data. The first paper dealt with the formulation of a single-Doppler radar TC wind retrieval technique, the ground-based velocity-track-display (GBVTD), and the results are verified using analytical TCs. It has been acknowledged that the quality of the GBVTD-retrieved TC circulation strongly depends on accurately knowing its center position. However, existing single-Doppler radar center finding algorithms are limited to estimate centers for axisymmetric TCs. The proposed algorithm uses a simplex method to objectively estimate the TC vorticity center by maximizing GBVTD-retrieved mean tangential wind.

When tested with a number of axisymmetric and asymmetric analytical TCs, the accuracy of the TC centers estimated by the GBVTD-simplex algorithm is ≈340 m from the true center. When adding 5 m s^{-1} random noise to the Doppler velocities, the accuracy of the TC centers is nearly unchanged at 350 m. When applying the GBVTD-simplex algorithm to Typhoon Alex (1987), the estimated uncertainty varies between 0.1 and 2 km. When the overall velocity gradient is weak, the uncertainties in the retrieved TC centers are usually large. The GBVTD-simplex algorithm sometimes has problems finding a solution when a large sector of Doppler radar data is missing in conjunction with weak velocity gradients.

The GBVTD-simplex algorithm significantly reduces the uncertainties in estimating TC center position compared with existing methods and improves the quality of the GBVTD-retrieved TC circulation. The GBVTD-simplex algorithm is computationally efficient and can be easily adapted for real-time applications.

1. Introduction

A number of methods have been used to identify tropical cyclone (TC) centers. These include 1) the geometric center defined as the center of TC eyewall radar reflectivity factor or clouds on satellite images (e.g., Griffin et al. 1992); 2) the wind center defined where the wind speed is zero (e.g., Wood and Brown 1992; Wood 1994); 3) the dynamic center defined as the minimum of the streamfunction, pressure, or geopotential height (e.g., Willoughby and Chelmow 1982; Dodge et al. 1999); and 4) vorticity (or circulation) center defined as the point that maximizes the eyewall vorticity (e.g., Willoughby 1992; Marks et al. 1992). All these centers may not be identified simultaneously from a particular observational platform and they are not necessarily collocated (Willoughby and Chelmow 1982). The uncertainties in estimating these centers range from a few kilometers to tens of kilometers in some extreme cases (e.g., Burpee and Marks 1984) and TC centers estimated by aircraft and radar are generally more accurate than those estimated from satellite images.

The uncertainties and inconsistencies of the estimated TC center on the order of 10 km may not pose serious problems in operational TC track forecasting; however, a few kilometers error in the estimated TC center position *critically* affects interpretation of the TC wind field in cylindrical coordinates. Willoughby (1992) demonstrated that a misplaced TC circulation center on an axisymmetric TC yielded an apparent wavenumber 1 gyre in the reconstructed streamfunction. Therefore, accurately knowing the circulation center of a TC is essential to partitioning the TC circulation into the ''azimuthal wavenumber'' (hereafter, referred to as ''wave-

* The National Center for Atmospheric Research is sponsored by the National Science Foundation.

Corresponding author address: Dr. Wen-Chau Lee, National Center for Atmospheric Research, P.O. Box 3000, Boulder, CO 80307. E-mail: wenchau@ucar.edu

number'') domain in a cylindrical coordinate system (Marks et al. 1992). In this context, the TC center is defined as the TC circulation (vorticity) center in this paper. Under this definition, the pressure center, vorticity center, and dynamic center of a TC are identical if the presence of multiple local minima within the eye are ignored (Willoughby and Chelmow 1982) and the streamfunction is nearly circular. However, the wind center and the geometric center may differ from the vorticity center owing to the vertical shear of the environment wind.

Using a simplex method (Nelder and Mead 1965), Marks et al. (1992) identified the vorticity center of Hurricane Norbert (1987) by maximizing the eyewall vorticity in a 10–15-km-wide annulus from the dual-Doppler radar derived winds in Cartesian coordinates. They also found that Norbert's centers varied with altitude owing to the vertical shear of the environmental wind. However, it is difficult to use the simplex method on ground-based single-Doppler radar data [e.g., the Weather Surveillance Radar-1988 Doppler (WSR-88D)] or airborne Doppler radar data [e.g., National Oceanic and Atmospheric Administration (NOAA) WP-3D] to objectively identify the TC center because TC circulation is not measured directly by a Doppler radar. At present, only centers of axisymmetric TCs can be objectively estimated from single-Doppler velocities (e.g., Wood and Brown 1992; Wood 1994; Harasti and List 1995). Recently, the development of the velocity track display (VTD; Lee et al. 1994) family of techniques, including extended VTD (EVTD; Roux and Marks 1996) and the ground-based VTD (GBVTD; Lee et al. 1999, hereafter referred to as Part I), enabled the TC axisymmetric and asymmetric circulations to be retrieved from single airborne or ground-based Doppler radar observations for a given TC center position. It is acknowledged that the quality of the retrieved TC circulation critically depends on accurately knowing the circulation center (Lee et al. 1994; Roux and Marks 1996; Part I) but this issue was not resolved in these papers.

This paper extends the work in Part I on applications of the GBVTD technique for TC center estimation, the GBVTD-simplex algorithm, from single-Doppler radar observations. Since the VTD family of techniques deduce axisymmetric and asymmetric tangential winds from single-Doppler velocities, it is feasible to combine the simplex method and the VTD-derived tangential circulation to identify the TC circulation center via an iterative process. The application of this algorithm is demonstrated using simulated Doppler velocities from analytical TCs constructed in Part I and data collected in Typhoon Alex (1987). The GBVTD technique is chosen here due to its wide-application potential to the WSR-88D network. The general results should hold for the VTD and EVTD techniques as well, where only the geometry is slightly different.

We will first examine the characteristics of the GBVTD-derived circulation using misplaced TC centers in section 2. Section 3 presents the computational procedure, the convergence criterion, and user-specified parameters. The performance and accuracy of the GBVTD-simplex algorithm is assessed using a number of analytical TCs in section 4. The results of the GBVTD-simplex algorithm applied to Typhoon Alex (1987) are presented in section 5. Section 6 discusses the factors affecting the accuracy of the GBVTD-simplex derived centers for real TCs. Conclusions are presented in section 7.

2. Characteristics of GBVTD analysis calculated with misplaced TC centers

It is instrumental to examine the characteristics of the GBVTD-derived circulation computed with a misplaced center. The purpose of this exercise is to establish the tolerable errors in estimating TC centers for discussions in sections 4–6. The knowledge base can be built by examining the GBVTD-retrieved circulation of axisymmetric and asymmetric analytical TCs when their estimated centers are misplaced in directions normal and parallel to the line connecting the radar and the TC center (hereafter, they are referred to as ''normal'' and ''parallel'' directions, respectively).

The analytical TCs contain a basic axisymmetric TC located at $x = 0.0$ km and $y = 60.0$ km in a Cartesian coordinate system [hereafter, all coordinates are in kilometers and relative to the radar located at (0.0, 0.0)] with a 50 m s^{-1} maximum axisymmetric tangential wind and a radius of maximum wind (RMW) of 20 km. Asymmetry was constructed by adding higher wavenumber tangential winds (with maximum amplitude of 10 m s^{-1} at RMW) to the axisymmetric vortex. A variety of asymmetric TCs ranging from wavenumber 1 to 3 were constructed and Doppler velocities were sampled by a hypothetical Doppler radar located at (0.0, 0.0). The raw Doppler velocities originally collected in a plane-position indicator (PPI) mode were interpolated onto a Cartesian grid (constant altitude PPI, CAPPI) with 1-km grid spacing, then interpolated onto a cylindrical grid with 1-km radial spacing centered at a given TC center. Finally, the TC tangential circulation is computed using the GBVTD technique.

The GBVTD-retrieved winds of the axisymmetric TC represented in the wavenumber domain are summarized in Table 1 as the estimated centers move away from the true center up to 5 km in both parallel and normal directions. The total tangential winds in both cases are illustrated in Fig. 1 (normal) and Fig. 2 (parallel), respectively. The total tangential wind is defined as the sum of the amplitude of all wavenumbers (relative tangential wind), plus the mean flow [see Eqs. (9) and (19)–(27) in Part I].

When the displacement of the TC center increases, the magnitude of the GBVTD-retrieved maximum axisymmetric tangential wind decreases and the RMW in-

TABLE 1. Amplitude of each wavenumber retrieved from the GBVTD analysis on different apparent centers. The true center is located at (0.0, 60.0). RMW is the radius that contains the highest wavenumber 0 (mean tangential wind). The original mean tangential wind at RMW has an amplitude of 50 m s^{-1}.

Apparent center (km)	Wave 0 (m s^{-1})	Wave 1 (m s^{-1})	Wave 2 (m s^{-1})	Wave 3 (m s^{-1})	Mean flow (m s^{-1})	RMW (km)
(0.0, 60.0)	48.2	0.0	0.0	0.0	0.0	20
(1.0, 60.0)	47.3	2.1	0.3	0.1	2.4	20
(2.0, 60.0)	45.5	6.4	0.8	0.3	4.5	21
(3.0, 60.0)	43.9	10.0	1.1	0.7	6.2	22
(4.0, 60.0)	42.6	12.6	1.5	0.7	7.5	23
(5.0, 60.0)	41.3	14.6	2.7	0.6	8.5	24
(0.0, 61.0)	48.0	2.1	0.7	0.2	0.0	20
(0.0, 62.0)	47.9	6.1	1.9	0.1	0.0	21
(0.0, 63.0)	47.6	7.8	3.0	0.0	0.0	21
(0.0, 64.0)	47.0	9.0	4.0	0.2	0.0	21
(0.0, 65.0)	46.2	10.1	4.8	0.4	0.0	21

creases slightly. An apparent wavenumber 1 asymmetry appears whose maximum is located in opposite direction of the displaced center (e.g., Fig. 2) and its magnitude increases as the displacement increases. These characteristics qualitatively agree with the findings in Willoughby (1992). The apparent wavenumber 1 amplitude is a function of both the axisymmetric tangential wind amplitude and the error in the TC center illustrated in Table 2.

Tropical cyclones, whose centers displaced in the normal direction (Fig. 1), seem to retain their axisymmetric wind pattern better than those cases where the center is displaced in the parallel direction (Fig. 2). Examining amplitudes of individual wavenumbers in Table 1 suggests that when the centers are displaced in the normal direction, not only the apparent wavenumber 1 amplitude is greater, but also an apparent mean flow is generated. These two components roughly cancel each other so the total tangential winds in Fig. 1 appear more axisymmetric than those in Fig. 2. In addition, the apparent circulation center is near the true center (×) rather than the displaced center (hurricane symbol). There is no apparent mean flow generated when centers are displaced in the parallel direction so the apparent wavenumber 1 dominates. These characteristics suggest that the GBVTD analysis attempts to satisfy the Doppler velocity pattern by manipulating individual wavenumbers to compensate for the misplaced TC center.

When the analytical TC has a true wavenumber 1 component, the resulting GBVTD-derived TC circulation becomes more interesting (Fig. 3). When the center is displaced toward the true wavenumber 1 maximum (Figs. 3b and 3c), the resolved wavenumber 1 amplitude is less than the true wavenumber 1 amplitude. When the center is displaced away from the true wavenumber 1 maximum, the resolved wavenumber 1 amplitude is greater than the true wavenumber 1 (Figs. 3d and 3e). These amplitude differences can be inferred from the area of the highest wind speed category and the error

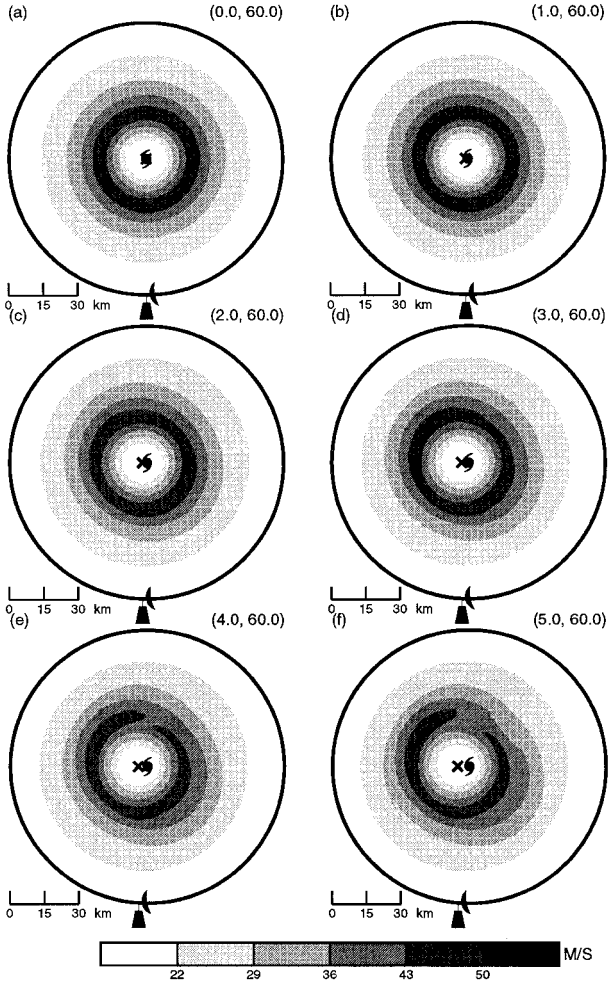

FIG. 1. The GBVTD-derived circulations from Doppler velocities sampled from an axisymmetric analytical TC at different estimated centers (hurricane symbol) displaced in the normal direction: (a) (0.0, 60.0), the control run; (b) (1.0, 60.0); (c) (2.0, 60.0); (d) (3.0, 60.0); (e) (4.0, 60.0); and (f) (5.0, 60.0). The true center (×) is located at (0.0, 60.0). Gray shades represent total tangential wind in m s^{-1}. Radar (radar symbol) is located at (0.0, 0.0).

increases as the displacement increases. When the center is displaced in the normal direction, the amplitude of the resolved wavenumber 1 is comparable to the true wavenumber 1 but the phase of the maximum changes slightly (Fig. 3f). As a result, a misplaced center will result in biases in both amplitude and phase of the retrieved wavenumber 1. Nevertheless, the wavenumber 1 asymmetry is unambiguously retrieved.

The amplitude of the apparent wavenumber 1 increases from 4% to 20% (4% to 29%) of the axisymmetric tangential wind when the center is displaced from 1 to 5 km from the true center in the normal (parallel) directions. However, when comparing these errors with a 10 m s^{-1} typical true wavenumber 1 amplitude, a 1- (2-) km deviation of the TC center produces 20% (60%) error. As a result, the effect of a misplaced center pro-

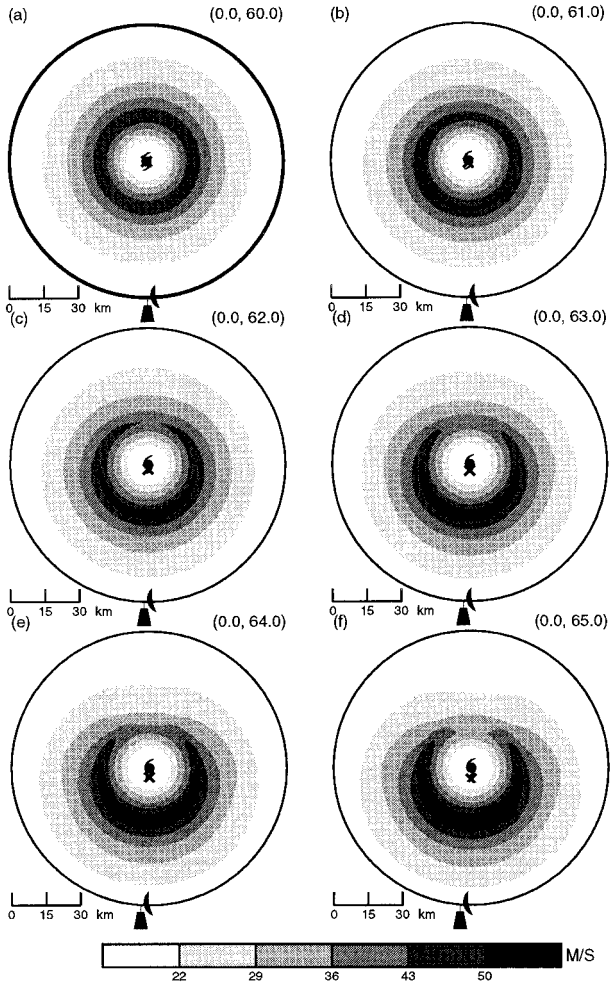

FIG. 2. Same as Fig. 1 but for different estimated centers displaced in the parallel direction: (a) (0.0, 60.0), the control run; (b) (0.0, 61.0); (c) (0.0, 62.0); (d) (0.0, 63.0); (e) (0.0, 64.0), and (f) (0.0, 65.0).

duces a more pronounced effect on the true wavenumber 1 amplitude than its axisymmetric amplitude. It is desirable to have the TC center known accurately within 1 km of the true center to keep the nominal error of the apparent wavenumber 1 $\leq$20% in the GBVTD analysis. This limit can be relaxed in weaker TCs because the absolute amplitude of apparent wavenumber 1 is proportional to the magnitude of the axisymmetric tangential wind as shown in Table 2.

3. The GBVTD-simplex TC center finding algorithm

The simplex method[1] (Nelder and Mead 1965) maximizes or minimizes a field (e.g., vorticity) in *n* dimen-

[1] The concept, equations, and a flowchart for function minimization of the simplex method are presented in Nelder and Mead (1965) with details for interested readers.

TABLE 2. The amplitude (m s^{-1}) of the apparent wavenumber 1 at the RMW (listed in Table 1) as a function of the TC intensity in terms of the axisymmetric tangential wind (first row) and different apparent TC centers (first column). The true TC center is (0.0, 60.0).

Cases	30 m s^{-1}	40 m s^{-1}	50 m s^{-1}	60 m s^{-1}
(0.0, 60.0)	0.0	0.0	0.0	0.0
(1.0, 60.0)	1.3	1.7	2.1	2.6
(2.0, 60.0)	3.8	5.1	6.4	7.6
(3.0, 60.0)	5.9	7.8	9.9	11.7
(4.0, 60.0)	7.5	10.0	12.5	15.0
(5.0, 60.0)	8.7	11.7	14.6	17.5
(0.0, 61.0)	1.2	1.7	2.1	2.6
(0.0, 62.0)	3.7	4.9	6.1	7.4
(0.0, 63.0)	4.6	6.2	7.8	9.3
(0.0, 64.0)	5.4	7.2	9.0	10.8
(0.0, 65.0)	6.0	8.1	10.1	12.1

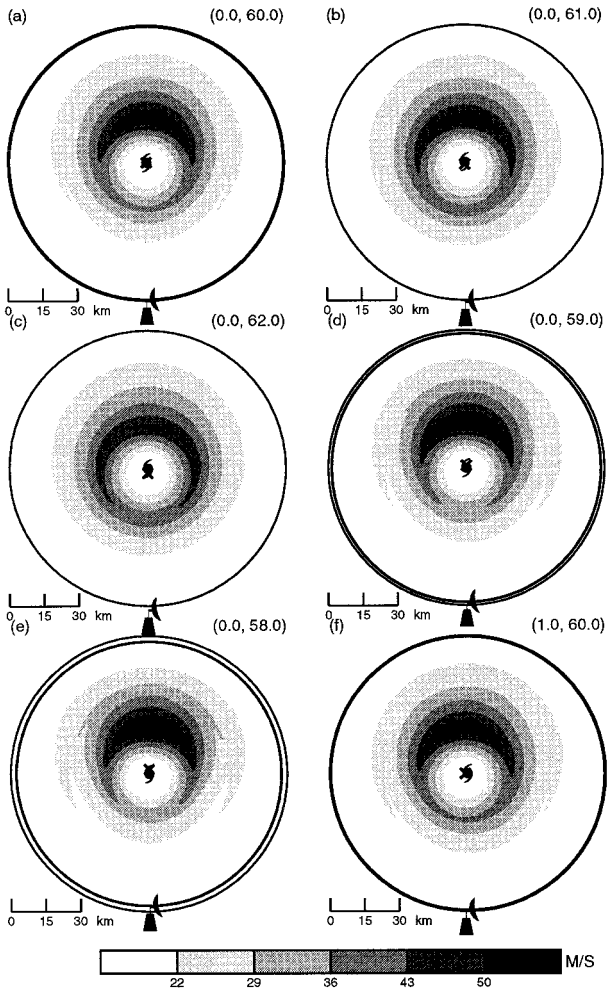

FIG. 3. The GBVTD-derived circulations from Doppler velocities sampled from a wavenumber 1 asymmetric analytical TC at different estimated centers (hurricane symbol): (a) (0.0, 60.0), the control run; (b) (0.0, 61.0); (c) (0.0, 62.0); (d) (0.0, 59.0); (e) (0.0, 58.0); and (f) (1.0, 60.0). The true center ($\times$) is located at (0.0, 60.0). Gray shades represent total tangential wind in m s^{-1}. Radar (radar symbol) is located at (0.0, 0.0). The inner circle in (d) and (e) indicates the outer limit of the GBVTD analysis at R = 58 and 59 km, respectively.

sions, by comparing function values at the $n + 1$ vertices of a general simplex, and replacing one of the vertices with the highest or lowest value of a new point. In a two-dimensional case ($n = 2$), a simplex is a triangle that contains three ($n + 1 = 3$) vertices whose centroid is the initial guess of the TC center. The simplex method uses three operations on a simplex—reflection, contraction, and expansion—to search for a new maximum or minimum in the field around the simplex. In the GBVTD-simplex algorithm, the field value at each vertex is computed from the GBVTD analysis on a Doppler velocity field using each vertex as the TC center. The GBVTD-simplex algorithm is initialized by providing the following parameters: 1) the initial guess of the TC center and the radius to form the initial simplex; 2) a radius interval for computation including the RMW; 3) the width of an annulus to evaluate the running mean of a field; 4) the coefficients for a simplex to reflect, expand, or contract; 5) the convergence criterion; and (6) the maximum number of iterations.

Based on earlier work (e.g., Willoughby 1992; Marks et al. 1992), there were two physical constraints that could be used for the convergence criterion in the GBVTD-simplex algorithm: 1) minimize eyewall wavenumber 1 amplitude, and 2) maximize eyewall wavenumber 0 amplitude (e.g., the vorticity). From the previous section, it is apparent that wavenumber 1 asymmetry is generated in an axisymmetric TC when the TC center is misplaced and the apparent asymmetry can be made to vanish by translating the TC center to a proper position (Willoughby 1992). The second criterion has been used to find the vorticity center of a TC (Marks et al. 1992). Both criterion were tested in all cases to evaluate their performance.

We use the following example (Fig. 4) to illustrate the GBVTD-simplex algorithm that finds the TC center possessing the highest mean tangential wind within an axisymmetric TC described in the previous section. The initial guess of the TC center, I, is (−10.0, 50.0) where the true TC center, hurricane symbol, is (0.0, 60.0). The computation is performed on radii from 15 to 25 km centered at the true RMW at $r = 20$ km. The radius to form the initial simplex is 4 km. The width of the annulus is 2 km, which is smaller than the 10–15-km width used in Marks et al. (1992). Using a smaller annulus tends to distinguish the maximum or minimum faster than using a larger width because the data is less smoothed. However, when missing data and noise become problems, one may need to increase the size of the annulus to include more data in the GBVTD analysis to better constrain the least squares curve fit.

The initial simplex is the triangle A–B–C with the centroid located at I, the initial guess of the TC center. The GBVTD-derived maximum mean tangential wind using each vertex as the TC center is listed in the parentheses beneath each point. Since vertex A has the lowest mean tangential wind (21.35 m s^{-1}), the first operation is to find a reflection point R1 of A on side

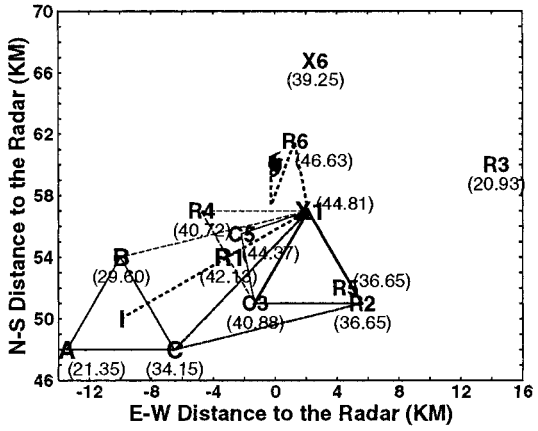

FIG. 4. Illustration of the GBVTD-simplex convergence path (thick dashed line) and the intermediate simplex from initial guess at I (−10.0, 50.0). Triangle A–B–C is the initial simplex with a centroid at I. Letters R, X, and C indicate the resulting points from reflection, expansion, and contraction operations with the number corresponds to individual simplex. The TC center is located at (0.0, 60.0) with a hurricane symbol. Only the first six iterations are shown here. The GBVTD-derived axisymmetric tangential winds are listed in parentheses in m s^{-1}. Different-shaped lines distinguish intermediate triangles.

BC. The reflection, expansion, and contraction coefficients are defined as 1.0, 1.0, and 0.5, respectively. These coefficients determine the distance of reflection, expansion, and contraction operations. The maximum mean tangential wind at R1 [VT(R1)] is evaluated and compared with those values at A, B, and C. Three conditions may occur: VT(R1) is either the maximum, minimum, or intermediate value compared with VT(A), VT(B), and VT(C). When VT(R1) is the maximum, as illustrated in this example, an expansion operation is executed and an expansion point X1 is found with VT(X1) = 44.81 m s^{-1}. Since VT(X1) $\geq$ VT(R1), X1 replaces A as one of the vertex of the second simplex B–C–X1. If VT(X1) $<$ VT(R1) or VT(R1) is an intermediate value, then R1 replaces A as the new vertex of the new simplex. This occurs in the second simplex. After finding the reflection point, R2, of B, VT(R2) is an intermediate value among VT(B), VT(X1), and VT(C), and R2 replaces B to form the third simplex C–X1–R2. When VT(R1) is a minimum, contraction operation is executed to find a contraction point. This occurs on the third simplex. When VT(R3) is a minimum, contraction point C3 is found and the fourth simplex, X1–R2–C3, is formed by replacing C with C3. If VT(C3) is smaller than VT(R3), a failed contraction occurred. This does not happen in our example. If a failed contraction occurs, the current simplex C–X1–R2 shrinks by moving C and R2 half the distance toward X1, the highest mean tangential wind among all three vertices, then restarting the process. The thick dashed line indicates the converging path of intermediate TC centers determined from the GBVTD-simplex algorithm. Note that the intermediate centers (e.g., at X1)

TABLE 3. The GBVTD-simplex-derived mean center locations on several axisymmetric and asymmetric TCs from 16 initial guesses that used minimizing wavenumber 1 as the convergence criterion. Also shown are the standard deviations of the 16 apparent centers (third column) and the resulting wavenumber 1 amplitude (last column). The true TC center is located at (0.0, 60.0) and the true amplitudes of wavenumbers 1, 2, and 3, are each 10 m s^{-1} at RMW.

Cases	Best-estimate center (km)	Std (km)	Mag. wave 1 (m s^{-1})
Sym. VT	(−0.131, 60.017)	0.023	0.05
Sym. VT + VR	(−0.112, 60.062)	0.028	0.07
Wave 1 at 0°	(3.393, 59.533)	0.028	0.07
Wave 1 at 45°	(3.377, 62.183)	0.025	0.08
Wave 1 at 90°	(−0.076, 64.630)	0.029	0.07
Wave 1 at 180°	(−3.380, 59.532)	0.021	0.07
Wave 1 at 270°	(−0.090, 56.306)	0.033	0.07
Wave 2 at 0°	(−0.492, 61.310)	0.083	0.09
Wave 2 at 90°	(−0.068, 58.518)	0.032	0.09
Wave 3 at 10°	(−0.178, 60.004)	0.023	0.06
Wave 3 at 90°	(−0.258, 60.028)	0.032	0.07

do not change from simplex 2 to 5 while the algorithm searches for the local gradient of the field. The intermediate centers converge to within 1 km of the true center in less than 10 iterations and it takes another 20–30 iterations to converge to the individual estimated center when all sides of the final simplex are smaller than 50 m.

4. Test on analytical TCs

In order to examine the sensitivity of the GBVTD-simplex algorithm to different initial conditions, a total of 36 points surrounding the true center of the analytical TC were used to initialize the GBVTD-simplex algorithm. These initial guesses are regularly spaced 4 km apart and fill a 20 km × 20 km square with the lower-left and upper-right corners located at (−10.0, 50.0) and (10.0, 70.0), respectively. So, the maximum error in the initial guesses is 14.1 km from the true center. Then, the best-estimated center is determined by averaging centers computed from all 36 runs while the standard deviation is used to detect possible outliers to be excluded in computing the final center. It takes about 10 s of CPU time on a Sun Ultra 1 workstation to run all 36 initial guesses for each radii. A typical operation tests about 10 radii in order to identify the best-estimate RMW at each altitude. For operational purposes, this computation can be done within 100 s for the lowest altitude. The actual computation time varies depending on parameters specified in section 3, the number of initial guesses, and the available computing resources.

Table 3 illustrates the results of the sensitivity tests that minimize the wavenumber 1 component as the convergence criterion (criterion 1). Using criterion 1, the algorithm always successfully finds a center that minimizes wavenumber 1 amplitude (close to zero in the last column of Table 3). For axisymmetric TCs, the results are very good, where the best-estimated TC centers are within 150 m of the true center in each run, in agreement with the theoretical derivation in Willoughby (1992). However, when a true wavenumber 1 asymmetry (10 m s^{-1} amplitude at RMW) exists, the GBVTD-simplex algorithm fails to converge to the true center or resolve the true wavenumber 1 amplitude. These results clearly demonstrate that an incorrect TC center not only creates an apparent wavenumber 1, but also modifies the true wavenumber 1 in the GBVTD analysis. The combined effect pushes the best center about 4–5 km toward the true wavenumber 1 maximum at $R = 20$ km, a result consistent with that shown in Fig. 3. Therefore, without knowing the amplitude and phase of the true wavenumber 1 in a real TC, minimizing the absolute wavenumber 1 magnitude (criterion 1) may provide misleading results.

TABLE 4. Same as Table 3 except that the GBVTD-simplex algorithm uses maximizing the eyewall vorticity as the convergence criterion. The last column is the resulting wavenumber 0 amplitude. The true wavenumber 0 amplitude at RMW is 50 m s^{-1}.

Cases	Best-estimated center (km)	Error (km)	Std (km)	Wave 0 (m s^{-1})
Sym. VT	(−0.01, 59.67)	0.31	0.137	48.9
Sym. VT + VR	(−0.18, 59.72)	0.33	0.085	48.8
Wave 1 at 0°	(0.09, 59.68)	0.34	0.049	48.8
Wave 1 at 45°	(0.06, 59.87)	0.15	0.069	47.0
Wave 1 at 90°	(−0.07, 59.96)	0.08	0.102	46.3
Wave 1 at 180°	(−0.24, 59.74)	0.35	0.097	49.0
Wave 1 at 270°	(0.04, 59.35)	0.65	0.166	51.4
Wave 2 at 0°	(−0.01, 59.85)	0.15	0.102	52.6
Wave 2 at 90°	(0.02, 59.37)	0.63	0.134	45.1
Wave 3 at 10°	(0.05, 59.75)	0.26	0.105	47.8
Wave 3 at 90°	(0.056, 59.49)	0.51	0.162	50.9
Mean error		0.34		

The mean errors of best-estimate centers in wavenumber 2 and 3 cases are 1.5 km and 300 m, respectively, which are better than those of the wavenumber 1 cases, but worse than those of the axisymmetric cases. This result is not surprising because there is no true wavenumber 1 component in the wavenumber 2 and 3 cases so they should perform better than the wavenumber 1 cases. The relatively large error in wavenumber 2 cases is due to the artificial wavenumber 1 component generated in the GBVTD analysis from the geometric distortion (discussed in Part I). Hence, characteristics similar to the wavenumber 1 cases appear.

Table 4 illustrates the results from convergence criterion 2, maximizing wavenumber 0 (the axisymmetric tangential wind). The mean error of the retrieved centers is 0.34 km from the true center with the worst standard deviation of 0.17 km. The mean error and standard deviation in each case are slightly higher than those using convergence criterion 1, but it is still well below the 1-km threshold determined in section 2. There are no significant differences in the accuracy of the retrieved center positions among axisymmetric and asymmetric TCs using convergence criterion 2. Therefore, it is con-

TABLE 5. Same as Table 4 except that a 5 m s^{-1} random noise is added to the velocity fields.

Cases	Best-estimate center (km)	Error (km)	Std (km)	Wave 0 (m s^{-1})
Sym. VT	(0.10, 59.65)	0.36	0.056	48.9
Sym. VT + VR	(0.09, 59.64)	0.37	0.067	48.9
Wave 1 at 0°	(0.10, 59.66)	0.35	0.040	48.9
Wave 1 at 45°	(0.11, 59.73)	0.29	0.046	47.1
Wave 1 at 90°	(0.11, 59.74)	0.28	0.061	46.4
Wave 1 at 180°	(0.07, 59.65)	0.37	0.143	49.0
Wave 1 at 270°	(0.09, 59.57)	0.44	0.08	51.5
Wave 2 at 0°	(0.10, 59.71)	0.31	0.067	52.7
Wave 2 at 90°	(0.09, 59.62)	0.39	0.046	45.2
Wave 3 at 10°	(0.10, 59.68)	0.34	0.051	47.9
Wave 3 at 90°	(0.10, 59.63)	0.38	0.162	51.0
Mean error		0.35		

cluded that maximizing the axisymmetric tangential wind is a robust constraint and should be used in the GBVTD-simplex TC center finding algorithm.

In order to simulate the sampling errors embedded in real data, random white noise ranging from ±1 to 5 m s^{-1} were added to the sampled Doppler velocity. The nominal Doppler velocity uncertainty of a ground-based radar is about 1 m s^{-1} (Wilson et al. 1984). Therefore, inserting a random error of 5 m s^{-1} represents a case with a 10% error to the maximum tangential wind of 50 m s^{-1} that easily exceeds the worst-case scenario. The results using Doppler velocity fields with 5 m s^{-1} random errors are illustrated in Table 5. The consistency between Table 4 and Table 5 illustrates that the GBVTD-derived best-estimated TC centers are not sensitive to white noise up to 5 m s^{-1}. This result is not surprising because the lower-order fit in the GBVTD analysis acts as a lowpass filter.

The standard deviations among all cases (using either constraints) are ≤200 m, indicating that the best-estimated centers identified by the GBVTD-simplex algorithm have little ambiguity. Therefore, the GBVTD-simplex algorithm is usually not sensitive to the location of the initial guess as long as it is within a reasonable range of the true center (14 km in this example). In nearly all situations, the errors in the best-estimated TC center from either aircraft or Doppler radar are very likely less than 14 km. As a result, we have demonstrated that the GBVTD-simplex TC center finding algorithm is very robust. In the next section, the GBVTD-simplex algorithm is tested using a real TC—Typhoon Alex (1987).

5. Application to Typhoon Alex

The computation procedure and results of the GBVTD-simplex algorithm applied to Typhoon Alex (1987) observed by the Civil Aeronautical Administration (CAA) Doppler radar are presented in this section. The CAA Doppler radar is a C-band operational radar located at the Chiang-Kai-Shek International Airport in northwestern Taiwan (marked by the radar symbol in Fig. 5) and its characteristics are summarized in Table 6. The CAA Doppler radar has a maximum range of 120 km for both reflectivity and Doppler velocity scanning in the Doppler mode and completes a 10-elevation-angle, 6-min volume scan every 15 min. The center of Alex entered CAA's Doppler range around 0400 LST (LST = UTC + 8) 27 July 1987. It made landfall on Taiwan about 0530 LST and reentered the East China Sea about 0800 LST. There were no observations between 0700 and 0917 LST due to a power outage at the CAA radar site. A total of 18 volumes of data before and after Alex's landfall in northern Taiwan were used to compute optimal TC circulation centers using the GBVTD-simplex algorithm.

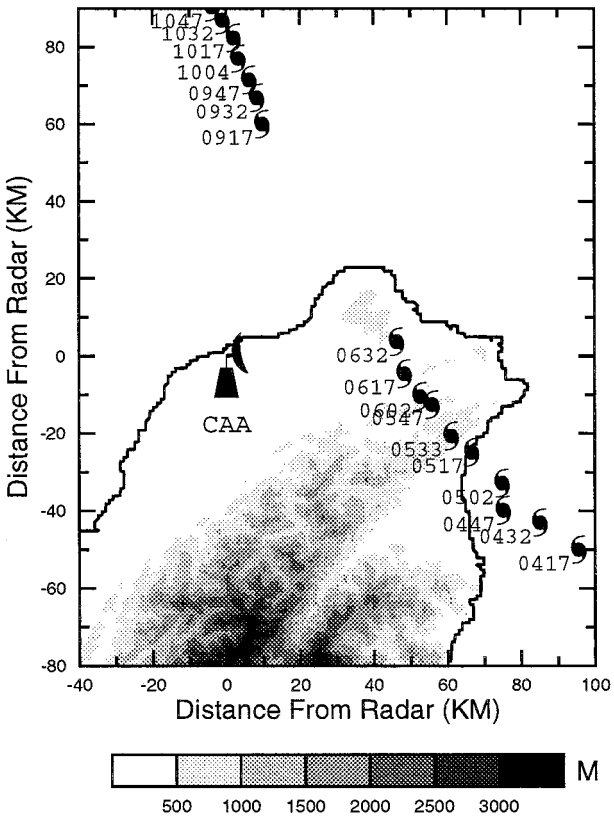

FIG. 5. The circulation centers of Typhoon Alex (z = 2 km) determined from the GBVTD-simplex algorithm from 0417 to 1047 LST 27 Jul 1987. Gray shades are the topography of northern Taiwan.

Typhoon Alex was the first typhoon observed by the CAA radar after its installation in April 1987. While capturing Alex moving across northern Taiwan and interacting with terrain (Fig. 5), this dataset includes a variety of conditions commonly observed in real TCs, such as different missing data patterns, different viewing angles from the radar as the TC moving across the radar scanning area, and intensity change (storm evolution). We intend to demonstrate, using Alex as an example, that physically plausible TC centers can be retrieved from the GBVTD-simplex algorithm. The evolution and

TABLE 6. The radar parameters and scanning strategy of the CAA Doppler radar.

Long	121.20°E	
Lat	25.07°N	
Altitude	27 m (MSL)	
Wavelength	5.31 cm	
Peak power	250 kW	
Antenna gain	43 db	
Beamwidth	0.85°	
Antenna polarization	Horizontal	
	Non-Doppler mode	Doppler mode
Pulse repetition frequency	250 Hz	900/1200 Hz
Unambiguous velocity	N/A	± 48 m s^{-1}
Unambiguous range	480 km	120 km
Pulse length	2 μs	0.5 μs
Receiver	Logarithmic	Linear
No. of samples	32	64
Minimum detectable signal	-109 dbm	-114 dbm
Range resolution	2 km	1 km
Ground-clutter suppression	$\geq$32 db	$\geq$26 db
Rotation rate	7.6 rpm	2.4 rpm
Elevation angles		0.5, 1.0, 1.5, 2.5, 3.5, 4.5, 6.0, 7.5, 10.0, 15.0

structure of Typhoon Alex are presented in Lee et al. (2000, manuscript submitted to *Mon. Wea. Rev.*, hereafter Part III).

The computation procedure is illustrated using the 0503 LST volume as an example. First, the initial center (hurricane symbol) at $x = 76.0$ km, $y = -24.0$ km and the RMW at 25 km at $z = 1$ km is specified by examining CAPPI reflectivity and Doppler velocity patterns (Fig. 6). A total of 16 initial centers in a 12 km $\times$ 12 km domain were chosen in a grid to start GBVTD-simplex computations. The computations were performed on 1-km intervals centered at the estimated RMW from R = 20 to R = 30 km. The GBVTD-simplex estimated center on each radius is the point that maximizes the eyewall axisymmetric vorticity or axisymmetric tangential wind. The best-estimated TC center was computed by averaging the estimated centers from all 16 runs at each radius (as apparent RMWs) and altitude. Then, centers that are one standard deviation away from the best-estimated center on each apparent RMW and altitude are discarded and the best-estimated TC center is recomputed by averaging the remaining points. Then, the best-estimated TC center and the best-estimated RMW are selected from the list that possesses the highest mean tangential wind among all apparent RMWs on each altitude. The final results (from $R = 20$–27 km) are illustrated in Table 7.

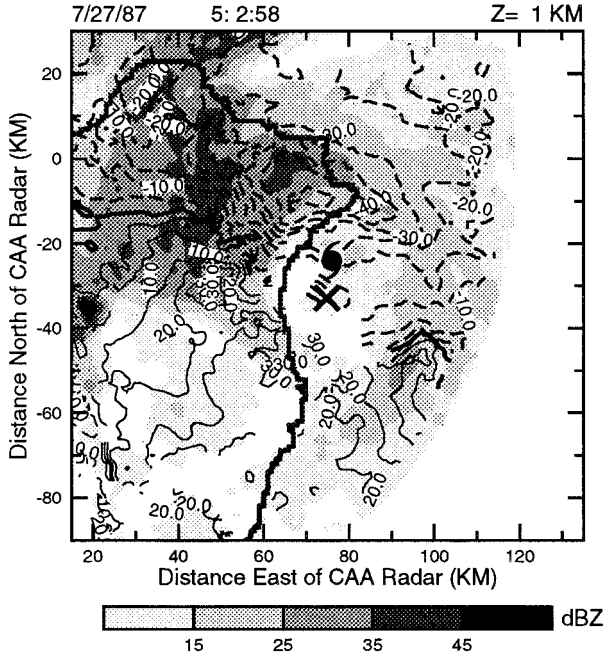

FIG. 6. The $z = 1$ km CAPPI display (0503 LST) of reflectivity factor (gray shades) and Doppler velocity of Typhoon Alex at 0503 LST. Solid (dashed) lines are positive (negative) velocities. Thick solid lines are zero Doppler velocities. Velocity interval is 5 m s^{-1}. The typhoon symbol is the initial guess of the TC center at (72.0, -24.0) while the $\times$ is the GBVTD-simplex-derived TC center at (72.1, -30.1). The thicker black solid line outlines Taiwan.

It is clear that the axisymmetric tangential wind at 1-km altitude monotonically increases from $R = 20$ km until $R = 23$ km, then it monotonically decreases beyond that radius. The maximum axisymmetric tangential wind of 38.28 m s^{-1} is located at $R = 23$ km and $z = 1$ km. Therefore, the best-estimated center for Alex at 0503 LST and 1-km altitude is (72.1, -30.1) with the best-estimated RMW of 23 km. The best-estimated TC center is obtained from averaging 13 out of 16 runs with a standard deviation of 0.1 km. This small standard deviation suggests a high confidence level on this center position. The GBVTD-retrieved relative tangential wind at $z = 1$ km and the axisymmetric tangential wind profile are illustrated in Fig. 7. The TC structures are plausible where high tangential winds coincide with the eyewall

TABLE 7. The best-estimate circulation center and the corresponding axisymmetric tangential wind for Typhoon Alex for different apparent RMWs. First, all 16 TC centers for each apparent RMW and altitude were computed. Then, centers that are beyond one standard deviation were rejected to obtain the final results in this table. The last column shows the number of points that are in the final computation. Standard deviations (fourth column) represent the scatter of these center estimates surrounding the final center.

Apparent RMW (km)	*H* (km)	Best-estimate cener (km)	Std (km)	Wave 0 (m s^{-1})	No. of points
20	1	(73.7, −28.6)	2.70	37.56	9/16
	2	(71.6, −28.1)	1.89	35.57	10/16
	3	(66.9, −28.4)	1.87	32.55	12/16
21	1	(68.8, −27.1)	1.37	37.98	13/16
	2	(72.2, −28.9)	2.29	35.85	8/16
	3	(72.0, −28.2)	3.51	32.63	8/16
22	1	(71.9, −29.9)	0.50	38.07	14/16
	2	(71.1, −30.0)	1.08	36.18	13/16
	3	(67.0, −27.2)	0.45	33.30	10/16
23	1	(72.1, −30.1)	0.10	38.28	13/16
	2	(71.8, −30.7)	1.51	36.56	13/16
	3	(69.4, −28.8)	4.06	33.46	6/16
24	1	(72.5, −31.2)	0.33	37.96	12/16
	2	(74.3, −32.3)	0.34	37.00	14/16
	3	(73.5, −32.8)	2.36	33.73	12/16
25	1	(73.2, −32.5)	0.59	37.90	13/16
	2	(74.1, −32.6)	0.19	37.01	12/16
	3	(73.0, −32.6)	0.56	34.10	13/16
26	1	(73.9, −33.2)	0.52	37.65	12/16
	2	(72.8, −33.2)	0.23	36.84	10/16
	3	(71.9, −32.7)	0.47	34.38	15/16
27	1	(73.4, −34.8)	0.30	37.34	10/16
	2	(72.5, −33.9)	0.17	36.52	9/16
	3	(72.8, −33.8)	0.34	34.59	15/16

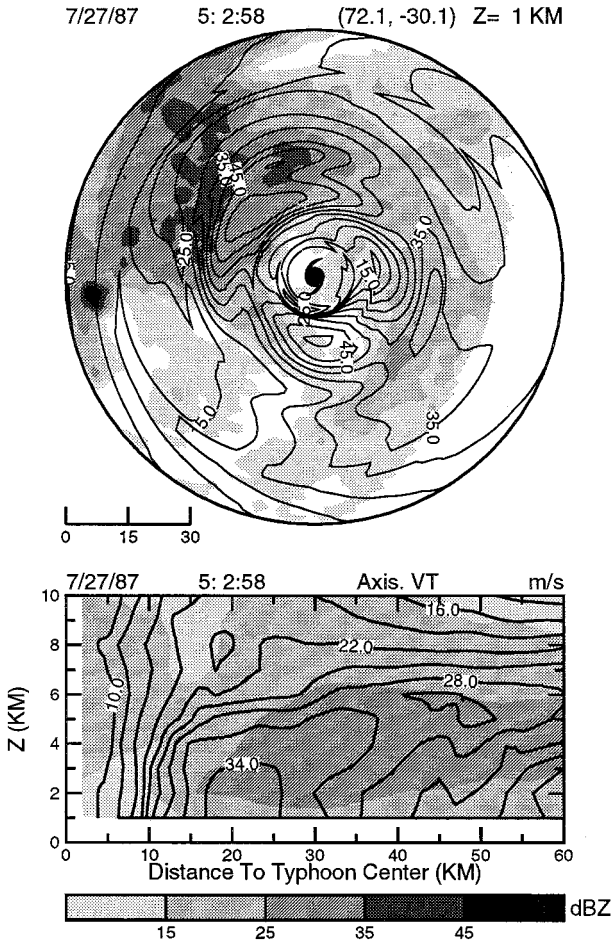

FIG. 7. The 0503 LST GBVTD-derived storm-relative tangential wind at $z = 1$ km (top panel) and the radius-height axisymmetric tangential wind (bottom panel). Reflectivity factor is in gray shades. Contour intervals are 5 m s^{-1} for the top panel and 3 m s^{-1} for the bottom panel.

convection (e.g., ring of high reflectivity) agreeing with previous TC studies (e.g., Marks et al. 1992). It is interesting to note that the highest radar reflectivity is located to the northwest of the TC center, which is likely the enhanced precipitation due to the interaction of Alex's circulation with terrain in northern Taiwan (Figs. 5, 6, and 7).

Note that the best center at $z = 2$ km is (−74.1, −32.6) and the RMW is 25 km while the center at $z = 3$ km is (72.8, −33.8) and the RMW is 27 km. This offset suggests that the center of Typhoon Alex varies with altitude, consistent with observations of other TCs (e.g., Marks et al. 1992). The increasing RMW with altitude is consistent with the outward sloping reflectivity maximum (Fig. 7). The standard deviations in Table 7 can be as high as 4 km. Higher standard deviations indicate increasing uncertainties in the TC center position and there are usually lesser points retained in the final computation as evident in the last column of Table 7. Careful examination of the results is necessary when the best-estimated center is accompanied by high standard deviations.

Typhoon Alex possessed a double eyewall structure shown in Fig. 8. From the Doppler velocity pattern, it suggests that the primary eyewall (associated with the maximum inbound and outbound Doppler velocities) has an RMW ≈25 km and a center at ≈(63.0, −16.0). The inner eyewall is characterized by a ≈5 km radius closed reflectivity loop that was not associated with local Doppler velocity extremes. The GBVTD-simplex algorithm finds the center at (61.9, −16.9) and a RMW of 23 km that is associated with the primary eyewall circulation. When testing apparent RMWs around 5 km, the GBVTD-simplex algorithm indicated a circulation center at (68.2, −27.4) with a 10 m s^{-1} axisymmetric tangential wind. Although the 10 m s^{-1} axisymmetric tangential wind is not a local maximum as defined in a conventional eyewall, the circulation center is consistent with the radius of the smaller radar reflectivity loop. At this time, Alex was over land and its circulation was disorganized by the influence of the terrain. It is not surprising that the primary and secondary centers do not coincide. This is a classic example where a single circulation center assumption breaks down. In order to retrieve the TC scale circulation, the TC center asso-

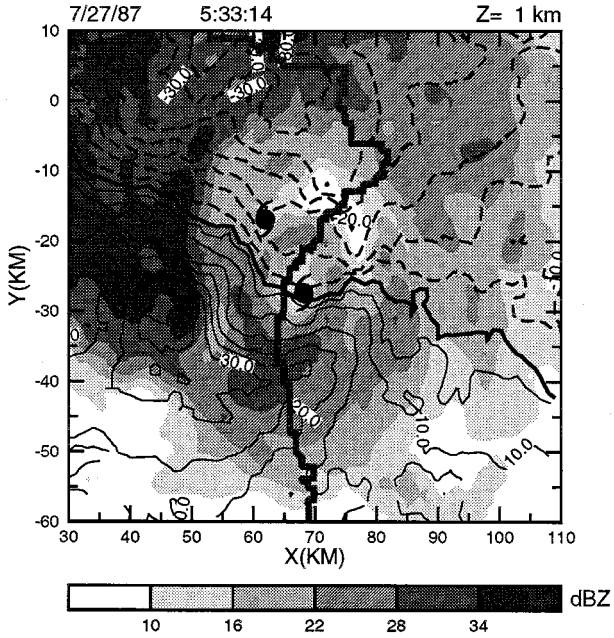

FIG. 8. The double eyewall structure of Typhoon Alex at 0533 LST and $z = 1$ km. The northern hurricane symbol indicates the GBVTD-simplex-derived TC center for the primary eyewall. The southern hurricane symbol indicates the GBVTD-simplex-derived TC center for the inner eyewall. Gray shades represent radar reflectivity. The Doppler velocity contour is every 5 m s^{-1}. Solid (dashed) lines are positive (negative) velocity. The thick solid line indicates 0 Doppler velocity. The thicker solid black line outlines Taiwan.

ciated with the primary eyewall needs to be used in the GBVTD analysis and one must realize that wind fields inside the primary eyewall may be questionable.

The centers of Typhoon Alex at 2-km altitude for over a 7-h period determined from the GBVTD-simplex algorithm are shown in Fig. 5. The TC center at 0647 LST could not be determined by the GBVTD-simplex algorithm because the circulation was disrupted and weakened by a 1-km-height mountain range resulting in multiple maxima and minima in the Doppler velocity field. In general, these independently determined TC centers are coherent within ≈1–2 km deviations to the mean north-northwest track. These deviations are an order of magnitude smaller than the trochoidal motions (e.g., Muramatsu 1986). Therefore, they are likely caused by either the terrain influences as Alex approached northern Taiwan and/or by the uncertainties in the GBVTD-simplex computation (e.g., large standard deviation). A more comprehensive study on typhoon tracks over northern Taiwan including other landfalling typhoons will be the subject of a future paper.

We have demonstrated that the GBVTD-simplex algorithm is not sensitive to where the initial guess is located (within a reasonable distance). For a fast-moving TC at 10 m s^{-1}, the center moves 3.6 km in 6 min (a typical WSR-88D volume scan) and 9 km in 15 min (a typical volume scan for CAA radar). These distances are within the range of initial guesses tested in this study. Therefore, when applying the GBVTD-simplex algorithm in real time, the best-estimated TC center on previous volume can be used as the initial guess for the current volume, hereby cutting down the computation time considerably (only one initial guess per altitude is needed).

6. Limitations of the GBVTD-simplex algorithm

In this paper, the GBVTD-simplex algorithm was described to identify TC centers with single-Doppler radar data. The mean error of the TC center determined by the GBVTD-simplex algorithm on analytical TCs has been shown to be 0.34 km. Because data were assumed perfect for analytical TCs, the error stems from the data smoothing effect by interpolation and coordinate transformation of the original Doppler radar data collected in PPI scans. It is also shown that the GBVTD-simplex-derived TC centers are not sensitive to random noise up to 5 m s^{-1}. We demonstrate that reasonable TC centers can be derived from the GBVTD-simplex algorithm under various conditions.

When the GBVTD-simplex algorithm was applied to TCs in real-time applications, additional problems in the Doppler radar data tend to degrade the results. These additional problems include but are not limited to 1) biases from ground clutter and second trip, 2) uneven data resolution due to beam spreading with range from the radar, 3) partial TC sampling due to limited unambiguous range, 4) missing data, and 5) velocity and range folding. Note that the Doppler radar data have been edited (nearly free of ground-clutter biases and range–velocity folding problems) before they are used in this study. In real-time applications, an automatic ground-clutter removal algorithm will be useful to remove the surface bias in the raw data. Recent development on range velocity ambiguity mitigation techniques (e.g., Keeler et al. 1999; Frush and Daughenbaugh 1999) will likely alleviate these aliasing problems in the future. There are no easy solutions for other problems. However, we have shown in Typhoon Alex that the GBVTD-simplex algorithm is quite robust with these biases embedded in the edited data.

It was found that the radial gradient of the mean tangential wind (or the Doppler velocity) is critical in determining the speed of convergence and the accuracy of the best-estimated center. When the radial gradient of the mean tangential wind is relatively flat as in most weak TCs, the simplex algorithm has difficulty pinpointing the exact maximum because the overall vorticity pattern changes little with each small vertex adjustment. Hence, the ambiguity of the best-estimated center increases as the radial gradient of the mean tangential wind weakens. In several time periods after 0917 LST in Typhoon Alex, the standard deviations associated with the best-estimated centers were around 1 km and can be as high as 2 km. Although amplitudes of the mean tangential winds are similar among these cen-

ters, the wavenumber 1 asymmetry may be quite different. In these situations, subjective adjustment of the best-estimated center based on the storm history and physical consistency on asymmetric structure (e.g., wavenumber 1) and RMW is sometimes needed to optimize the overall circulation and storm continuity.

Missing data (or unevenly distributed data) in a random pattern is usually not a problem because the GBVTD technique relies on a least squares curve fit, not the absolute maximum and minimum, to retrieve TC wind fields. However, when combining extensive missing data with a weak velocity gradient, the GBVTD-simplex algorithm may not converge to a solution. This problem usually occurs at upper levels of a weak TC when the coverage of the TC in CAPPIs is limited near the radar, the primary reason why the center computations were only performed up to $z = 3$ km in Typhoon Alex.

Unfortunately, it is nearly impossible to assess the accuracy of the GBVTD-simplex algorithm-retrieved TC centers in Typhoon Alex because there was no aircraft reconnaissance in the western Pacific basin. The quality of the TC center can only be judged by examining the GBVTD-retrieved circulation for physical consistency as we demonstrated in section 5 and storm continuity (in Part III).

7. Conclusions

The GBVTD-simplex algorithm is presented to objectively identify the TC circulation center from single-Doppler radar observations. Maximizing the mean tangential winds (i.e., eyewall vorticity) is demonstrated as a more robust convergence criterion compared with minimizing the absolute wavenumber 1 amplitude within the eyewall. The GBVTD-simplex algorithm finds best-estimated TC centers within 0.34 km of the true center in a number of axisymmetric and asymmetric analytical TCs. In applying the GBVTD-simplex algorithm to Typhoon Alex, the accuracy is sometimes degraded to 2 km due to a combination of missing data and weak velocity gradients. Except for the unstable situations described in section 6, the estimated uncertainty of the GBVTD-simplex-determined best-estimated center is comparable to the 1-km limit (section 2), suitable for operational and most research purposes. For research purposes that require a higher accuracy of the wind field, these GBVTD-simplex-estimated TC centers may need to be further examined in conjunction with the physical consistency and storm continuity of the GBVTD-retrieved wind fields. Some subjective fine-tuning of the GBVTD-simplex-estimated TC centers may be required to improve the results.

The GBVTD-simplex algorithm is computationally efficient. The procedure can be automated such that the initial guess is assigned as the TC center in the previous volume or estimated from the method outlined in Wood and Brown (1992) and Wood (1994). Therefore, it is feasible to use the GBVTD-simplex algorithm in real time at the National Hurricane Center located in Miami, Florida, to determine the TC circulation center during landfalling TC events in addition to the centers determined from aircraft reconnaissance and satellite. The relationship between the GBVTD-simplex-determined vorticity centers and aircraft-derived wind center needs further investigation using Atlantic landfalling hurricanes where routine aircraft reconnaissance is available.

Although the GBVTD-simplex algorithm, in conjunction with the simple vorticity convergence criterion, has performed quite satisfactorily in a relatively weak typhoon under strong terrain influences, more case studies are needed to better understand its performance on a spectrum of TCs on various intensity and data distributions. The GBVTD-simplex algorithm provides the basic framework where more complex convergence criteria may be implemented and tested in the future.

Acknowledgments. The first author thanks NOAA/AOML/HRD for hosting a three-month sabbatical leave where most of the work was completed. The authors are grateful to Dr. Peter Hildebrand, Mr. Scott Ellis, Dr. Frank Roux, Dr. Tammy Weckwerth, and two anonymous reviewers for their valuable comments that greatly improved this paper. Ms. Jennifer DeLaurant proofread the manuscript. Typhoon Alex's data was provided by the CAA Doppler radar. This research was partially supported by the National Science Foundation and the National Oceanic and Atmospheric Administration.

REFERENCES

Burpee, R. W., and F. D. Marks Jr., 1984: Analyses of digital radar data obtained from coastal radars during Hurricane David (1979), Frederic (1979), and Alicia (1983). Preprints, *10th Conf. on Weather Forecasting and Analysis,* Clearwater Beach, FL, Amer. Meteor. Soc., 7–14.

Dodge, P., R. W. Burpee, and F. D. Marks Jr., 1999: The kinematic structure of a hurricane with sea level pressure less than 900 mb. *Mon. Wea. Rev.,* **127,** 987–1004.

Frush, C. L., and J. Daughenbaugh, 1999: Range/velocity ambiguity reduction: Evaluation of the SZ(8/64) phase code on a WSR-88D radar. Preprints, *29th Int. Conf. on Radar Meteorology,* Montreal, PQ, Canada, Amer. Meteor. Soc., 513–516.

Griffin, J. S., R. W. Burpee, F. D. Marks Jr., and J. L. Franklin, 1992: Real-time airborne analysis of aircraft data supporting operational hurricane forecasting. *Wea. Forecasting,* **7,** 480–490.

Harasti, P. R., and R. List, 1995: A single-Doppler radar analysis method for intense axisymmetric cyclones. Preprints, *27th Conf. on Radar Meteorology,* Vail, CO, Amer. Meteor. Soc., 221–223.

Keeler, R. J., D. S. Zrnic, and C. L. Frush, 1999: Review of range velocity ambiguity mitigation techniques. Preprints, *29th Int. Conf. on Radar Meteorology,* Montreal, PQ, Canada, Amer. Meteor. Soc., 158–163.

Lee, W.-C., F. D. Marks, and R. E. Carbone, 1994: Velocity Track Display—A technique to extract real-time tropical cyclone circulations using a single airborne Doppler radar. *J. Atmos. Oceanic Technol.,* **11,** 337–356.

——, B. J.-D. Jou, P.-L. Chang, and S.-M. Deng, 1999: Tropical cyclone kinematic structure retrieved from single Doppler radar observations. Part I: Interpretation of Doppler velocity patterns and the GBVTD technique. *Mon. Wea. Rev.,* **127,** 2419–2439.

Marks, F. D., R. A. Houze, and J. F. Gamache, 1992: Dual-aircraft investigation of the inner core of Hurricane Norbert. Part I: Kinematic structure. *J. Atmos. Sci.*, **49,** 919–942.

Muramastsu, T., 1986: Trochoidal motion of the eye of Typhoon 8019. *J. Meteor. Soc. Japan,* **51,** 475–485.

Nelder, J. A., and R. Mead, 1965: A simplex method for function minimization. *Comput. J.,* **7,** 308–313.

Roux, F., and F. D. Marks, 1996: Extended Velocity Track Display (EVTD): An improved processing method for Doppler radar observations of tropical cyclones. *J. Atmos. Oceanic Technol.,* **13,** 875–899.

Willoughby, H. E., 1992: Linear motion of a shallow-water barotropic vortex as an initial-value problem. *J. Atmos. Sci.*, **49,** 2015–2031.

——, and M. B. Chelmow, 1982: Objective determination of hurricane tracks from aircraft observations. *Mon. Wea. Rev.,* **110,** 1298–1305.

Wilson, J. W., R. D. Roberts, C. Kessinger, and J. McCarthy, 1984: Microburst wind structure and evolution of Doppler radar for airport wind shear detection. *J. Climate Appl. Meteor.,* **23,** 898–915.

Wood, V. T., 1994: A technique for detecting a tropical cyclone center using a Doppler radar. *J. Atmos. Oceanic Technol.,* **11,** 1207–1216.

——, and R. A. Brown, 1992: Effects of radar proximity on single-Doppler velocity signatures of axisymmetric rotation and divergence. *Mon. Wea. Rev.,* **120,** 2798–2807.